

Introducing Perturb-ability Score (PS) to Enhance Robustness Against Evasion Adversarial Attacks on ML-NIDS

Author's draft for soliciting feedback: 5 Nov. 2024

Mohamed elShehaby
 Carleton University
 Ottawa, Canada
 mohamedelshehaby@cmail.carleton.ca

Ashraf Matrawy
 Carleton University
 Ottawa, Canada
 ashraf.matrawy@carleton.ca

Abstract—As network security threats continue to evolve, safeguarding Machine Learning (ML)-based Network Intrusion Detection Systems (NIDS) from adversarial attacks is crucial. This paper introduces the notion of *feature perturbability* and presents a novel *Perturb-ability Score (PS)* metric that identifies NIDS features susceptible to manipulation in the problem-space by an attacker. By quantifying a feature's susceptibility to perturbations within the problem-space, the PS facilitates the selection of features that are inherently more robust against evasion adversarial attacks on ML-NIDS during the feature selection phase. These features exhibit natural resilience to perturbations, as they are heavily constrained by the problem-space limitations and correlations of the NIDS domain. Furthermore, manipulating these features may either disrupt the malicious function of evasion adversarial attacks on NIDS or render the network traffic invalid for processing (or both).

This proposed novel approach employs a fresh angle by leveraging network domain constraints as a defense mechanism against problem-space evasion adversarial attacks targeting ML-NIDS.

We demonstrate the effectiveness of our PS-guided feature selection defense in enhancing NIDS robustness. Experimental results across various ML-based NIDS models and public datasets show that selecting only robust features (low-PS features) can maintain solid detection performance while significantly reducing vulnerability to evasion adversarial attacks. Additionally, our findings verify that the PS effectively identifies NIDS features highly vulnerable to problem-space perturbations.

1. Introduction

In the contemporary landscape of cybersecurity, Machine Learning (ML) has emerged as a cornerstone technology for Network Intrusion Detection Systems (NIDS). The ability of ML algorithms to process and classify vast amounts of network traffic data with high accuracy makes them indispensable for identifying malicious activities and safeguarding network integrity [1] [2]. However, the effectiveness of ML-based systems is challenged by adversarial attacks, which exploit vulnerabilities in the ML models to fool their detection mechanisms [3]. There are multiple types of adversarial attacks, such as poisoning

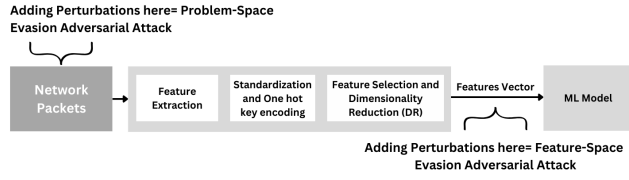


Figure 1. Evasion Adversarial Attacks in Feature-Space vs Problem-Space Against NIDS

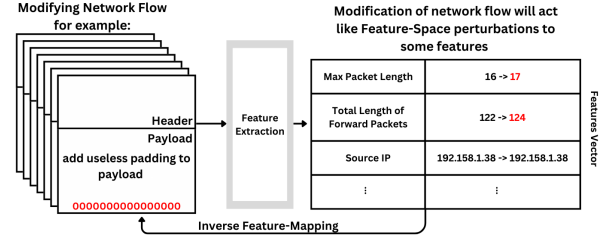


Figure 2. Example of Evasion Adversarial Attacks Problem-Space Perturbations Against NIDS

[4], backdoor [5], model stealing [6], and evasion attacks, which are the main focus of this paper.

Evasion adversarial attacks involve the strategic manipulation of input data to deceive the ML model into making incorrect classifications. These perturbations are often crafted using gradients derived from the target model, allowing attackers to subtly alter the input while maintaining its functionality from a network perspective.

1.1. Feature-Space vs Problem-Space Evasion Adversarial Attacks Against ML-NIDS

It is crucial to differentiate between feature-space and problem-space (real-world objects) in ML [7]. Feature-space refers to the representation of input data as features used by the ML model, while problem-space refers to the raw input data before feature extraction. Ibitoye et al. [3] introduced the concept of 'space' in their taxonomy of adversarial attacks for network security, distinguishing between feature-space and problem-space attacks. **Feature-space adversarial attacks** manipulate or perturb feature vectors, assuming that the attacker can directly access and alter these features; however, this assumption is often unrealistic in practical scenarios. In contrast, **problem-**

space adversarial attacks modify or perturb actual data, such as network traffic (e.g., adding delays) or packets (e.g., padding the payload), which attackers typically can access. Fig. 1 illustrates this distinction.

Feature-space attacks may not be practical against NIDS due to challenges an attacker would face in feature vector access and challenges with feature correlations and network constraints [1]. On the other hand, problem-space attacks are more practical than feature-space as the modifications happen to the network packets (feasible for an external attacker). They typically start with feature-space perturbations, then translate to real-world packet modifications (Inverse Feature-Mapping [8]). In other words, as seen in Fig. 2, attackers modify the adversarial network flow to produce perturbations in certain targeted features within the feature vector after feature extraction. Fig. 2 illustrates an example of evasion adversarial attack problem-space perturbations against NIDS, where the attacker adds padding to the payload of a packet to perturb features such as the maximum packet length and total length of forward packets in the feature vector. Despite being considered more practical than feature-space attacks, these attacks also face several practicality issues [1] [9] [10], such as: challenges in maintaining malicious objective and network functionality while altering packets; keeping up-to-date knowledge of the model, its features, and extraction techniques; or predicting correct common features. Problem-space attacks must also address NIDS features constraints.

1.2. Perturb-ability of Features in Problem-Space Against NIDS

Problem-space evasion attacks on NIDS [11]–[18] involve modifying network packets to manipulate certain features within the feature vector. Perturbing some NIDS features in the problem-space without affecting network functionality might be feasible; for instance, adding padding to payloads or introducing delays between packets can perturb features such as length and interarrival time (Fig. 3a). However, problem-space constraints significantly limit the perturb-ability of many other NIDS features. For example, modifying the destination IP or port number disrupts the malicious capability or network functionality of the flow (Fig. 3b), and certain features, like backward and inter-flow/connection features, are inaccessible for modification.

To address this distinction, we coined the terms “perturb-able” and “non-perturb-able” features. A perturb-able feature refers to a feature that can be altered through problem-space modifications without affecting the attacker’s malicious capability or violating network constraints. Non-perturb-able, or robust, features, on the other hand, cannot be perturbed through such modifications without disrupting the malicious capability or network constraints. Fig. 3 shows examples of perturb-able and non-perturb-able features in network traffic.

N.B. Some non-perturb-able (or robust) features may be completely unmodifiable due to problem-space limitations and correlations within the NIDS domain. For example, some backward features (features describing the network flow from server to client), like the mean size of a packet in the backward direction feature, can be

extremely difficult for an attacker to access. However, it is important to note that most features can be modified through problem-space manipulations. By non-perturbable features, we specifically refer to those that cannot be perturbed in the problem space **while maintaining the attacker’s malicious aim and complying with NIDS domain constraints**. For instance, changing the destination IP to manipulate its corresponding feature in the feature vector is possible. However, doing so would disrupt the flow’s network functionality and the attacker’s malicious objective, which is why we classify it as a non-perturbable feature.

1.3. Motivation and Aim

Our motivation stems from the intuitive assumption that attackers can only access the problem-space rather than the feature-space. This perspective aligns with the reality of most network environments, where attackers can manipulate packet contents but do not have direct control over the feature extraction process (see §2 for more details on our threat model).

In response to this, our aim is to introduce the novel notion of the Perturb-ability Score (PS) metric, which is designed to enhance the robustness of ML-based NIDS. The PS metric helps to identify features in the problem-space that are susceptible to manipulation by attackers, without compromising the malicious functionality of network traffic. By quantifying the perturb-ability of each feature within NIDS domain constraints, PS facilitates the selection of features that are inherently more resistant to adversarial attacks. Our aimed classification is shown in Fig. 4. For the remainder of the paper, we will use the color scheme found in Fig. 4, i.e., a green feature represents a feature in the Low Perturb-ability class, a yellow feature represents a feature in the Medium Perturb-ability class, and a red feature represents a feature in the High Perturb-ability class.

Our approach embodies this philosophy by offering a straightforward yet highly effective defense against evasion adversarial attacks targeting ML-based Network Intrusion Detection Systems (ML-NIDS). What sets our solution apart is its independence from attack types, attack-norms [19] used, or the level of adversarial knowledge (whether black-box, white-box, or gray-box [3]).

Unlike most conventional defenses that focus primarily on the internal mechanisms of the ML model itself our method takes an “*outside-the-box*” perspective. By leveraging inherent network domain constraints external to the ML model, we significantly reduce the attack surface. This strategic shift from model-centric defenses to exploiting network domain properties introduces a novel layer of protection, enhancing the overall robustness of ML-NIDS against adversarial threats.

In this paper, we demonstrate the efficacy of PS-guided feature selection in fortifying ML-based NIDS against adversarial attacks. Through extensive experiments on various NIDS models and public datasets, we show that PS-selected features maintain solid detection performance while significantly reducing vulnerability to adversarial manipulations. By “maintain solid detection performance,” we mean that the difference in performance metrics between the ML-NIDS model trained exclusively

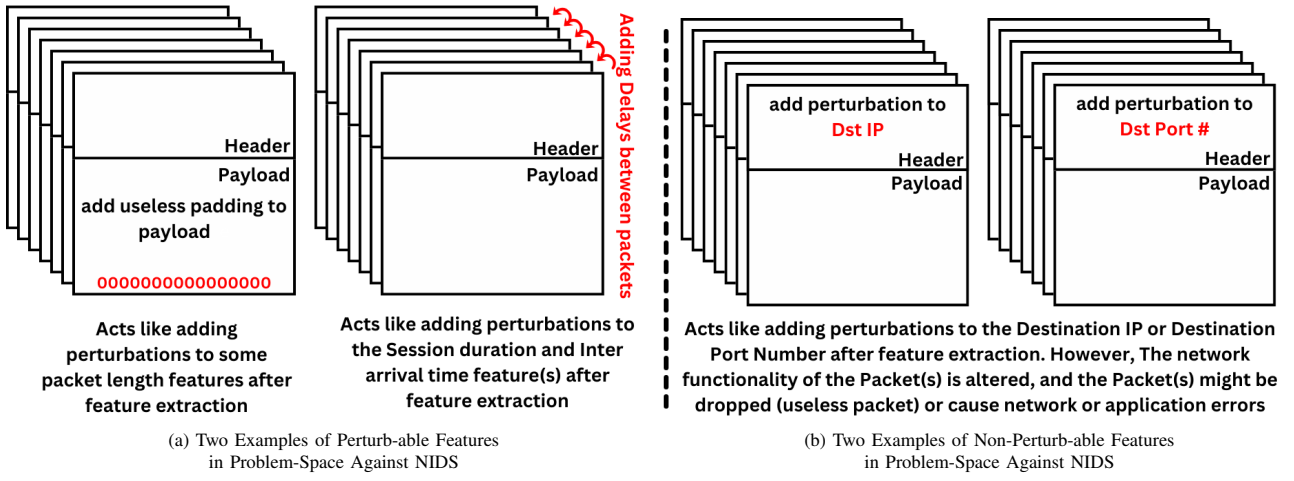


Figure 3. Examples of Perturbable vs Non-Perturbable Features in Network Traffic

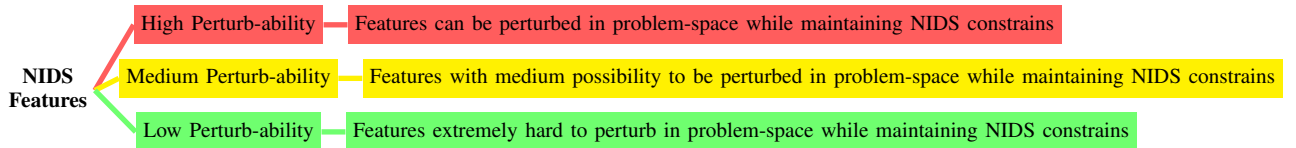


Figure 4. Classification of NIDS Features based on our proposed PS, where green represents a feature in the Low Perturbability class, yellow represents a feature in the Medium Perturbability class, and red represents a feature in the High Perturbability class

on non-perturbable (robust) features and the ML-NIDS model trained on all features is minor.

This work represents a promising step towards developing resilient NIDS capable of withstanding the evolving threat landscape.

1.4. Contributions

Our contributions are threefold: (1) **Introduction of Perturbability Score (PS) (§3)**: We propose a novel Perturbability Score (PS) metric to quantify the vulnerability of NIDS features to adversarial manipulation. The PS measures the susceptibility of a feature to perturbation by an attacker without compromising the underlying malicious objective or network functionality of the attack. This metric establishes a robust foundation for assessing feature robustness in ML-NIDS adversarial contexts. (2) **Leveraging PS as a Defensive Mechanism (§3.4)**: By utilizing PS, we introduce a defense strategy that enhances the robustness of ML-based NIDS. PS-guided feature selection enables the identification of inherently resilient features that remain robust against adversarial perturbations. This approach fortifies NIDS by reducing the attack surface while maintaining solid detection performance across various models and datasets. (3) **Mapping Problem-Space Adversarial Attacks to feature-space (§5.4)**: We conduct an in-depth analysis of problem-space adversarial attack techniques found in literature by mapping their traffic morphing methods to the corresponding NIDS features. This mapping validates the PS classification, demonstrating how PS effectively captures the impact of problem-space evasion techniques on NIDS features and provides significant insights into how adversarial attacks manifest in both problem and feature-spaces.

2. Threat Model of a “Practical” Evasion Adversarial Attack Against NIDS

In this section, we describe what we consider a threat model for a practical evasion adversarial attack against NIDS.

Despite the critical importance of defending against adversarial attacks, much of the existing research has focused on computer vision datasets, where the primary objective is to fool human perception [20]. This focus has led to the development of algorithms optimized for visual data, which may not directly translate to the network security domain. Furthermore, many studies on adversarial attacks against ML-NIDS operate under the assumption that adversaries have full control over the feature-space, an unrealistic scenario in practical settings [7].

Attacker’s Knowledge: In a practical setting, we assume that the attacker has no knowledge (black-box attack) of the following: training data, selected features (feature vector), feature extractor, feature transformers, ML algorithm, activation functions, parameters, hyperparameters, and confidence intervals. Moreover, we assume that the attackers have no access to model outputs (i.e., they cannot query the model).

Attacker’s Capability: We assume that the attacker has no access to the feature vector. In this scenario, the attacker has access to and can only alter network packets (problem-space attack). To bypass detection, they must craft these adversarial packets while adhering to several constraints: (1) **Maintaining Functionality**: Malicious capability must be preserved alongside the network functionality of the packets. (2) **NIDS Feature Constraints**: The attacker needs to consider the feature limitations of the NIDS model. These constraints might involve specific

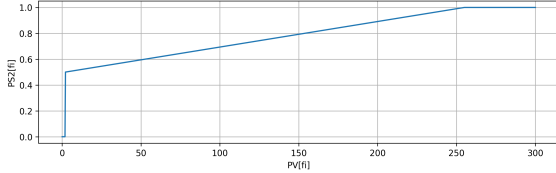


Figure 5. Visualization of the $PS_2[f_i]$ Evaluation Equation

data formats, packet sizes, correlations, or limitations on certain network protocols.

Attacker’s Goal: The attacker’s main objective is to compromise the integrity of the NIDS by evading detection (evasion adversarial attacks) while maintaining malicious and network functionalities of the perturbed network flow.

Such a threat model might be infeasible, as recent research studies have cast doubt on the practicality of evasion adversarial attacks against NIDS [1] [21] [22]. However, in this paper, we focus solely on the possibility and implications of adding perturbations to NIDS features in the problem-space. Therefore, we will assume that such a threat model is feasible for an extremely powerful attacker.

3. Perturb-ability Score (PS)

In this section, we explain how our novel Perturbability Score (PS) quantifies the susceptibility of each feature to perturbation and facilitates defense against practical problem-space evasion attacks.

3.1. NIDS Features Perturb-ability Classification

The aim of our perturb-ability Score (PS) is to classify NIDS features based on their susceptibility to perturbations within the problem-space while adhering to NIDS constraints. By NIDS constraints, we refer to the problem-space constraints within the NIDS domain, including the limitations, correlations, and restrictions inherent to network traffic and NIDS attacks. This classification is crucial for understanding the robustness of NIDS against evasion adversarial attacks and may be utilized as a defense, as we will discuss later in this paper. As seen in Fig. 4, our PS aims to categorize features into three main groups: high Perturb-ability, medium Perturb-ability, and low Perturb-ability.

High Perturb-ability features (high PS) can be perturbed in the problem-space while adhering to NIDS domain constraints, such as the maximum inter-arrival time (IAT) between packets in the forward direction (from client to server). In contrast, low Perturb-ability features are difficult or extremely difficult to perturb while maintaining these constraints, like the destination IP. Medium Perturb-ability features fall between these two extremes.

3.2. Evaluating PS

The goal of PS is to obtain a Perturb-ability score for each feature (f_i) in a dataset D , where i is the ID of the feature from 1 to n , and n is the number of features in D . PS should range from 0 (features extremely hard to

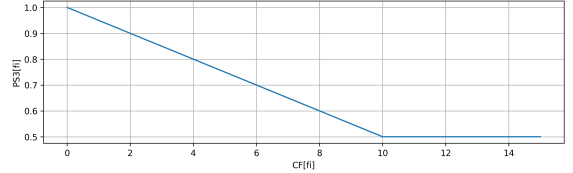


Figure 6. Visualization of the $PS_3[f_i]$ Evaluation Equation

perturb in problem-space while maintaining the networks constraints) to 1 (features can be perturbed in problem-space while maintaining the networks constraints). The $PS_{Total}[f_i]$ is the geometric average of the following five fields:

3.2.1. $PS_1[f_i]$: Strict Header Features/ Affects Network or Malicious Functionality. This PS field focuses on strict Header features and network/malicious functionality of network flows after adding perturbations in the problem-space. $PS_1[f_i]$ will be 0 if any of the following conditions are true (which will make $PS_{Total}[f_i]$ equals 0);

C1: the feature f_i is a strict header feature (IP addresses in TCP flows, destination port number or protocol)

C2: adding perturbation to feature f_i will affect the network or malicious functionality of the flow.

$PS_1[f_i]$ can be described with the following equation:

$$PS_1[f_i] = \begin{cases} 0, & \text{if (C1 or C2)} \\ 1, & \text{otherwise} \end{cases}$$

3.2.2. $PS_2[f_i]$: The range of Possible Values of a Feature. This PS field considers the cardinality (number of possible values) of a NIDS feature. In unconstrained domains like computer vision, attackers can freely perturb pixels, which typically have a range of 0 to 255 per channel (e.g., red, green, blue). Conversely, certain NIDS features have limited cardinality. For example, a NIDS dataset may have binary or categorical features with a limited number of categories. Such features offer less flexibility to attackers. The gradients of the targeted model might suggest perturbations in a specific direction, but the attacker might be unable to comply due to the limited number of possible feature values of these features.

$PS_2[f_i]$ will be 1 if f_i ’s number of Possible Values (PV) is greater than 255 (this feature will be similar to computer vision’s pixel, and it will be flexible to perturb). On the other hand, if f_i ’s PV ($PV[f_i]$) is less than or equal to 255, $PS_2[f_i]$ will be equal to a linear function where its output is 1 if f_i ’s PV is 255, and 0.5 if f_i ’s PV is 2 (binary). If $PV[f_i]$ is less than 2 (equals 1), it indicates that f_i is non-perturbable, in which case $PS_2[f_i]$ will be set to 0. However, in this case (where $PV[f_i]$ equals 1), we recommend dropping that feature, as it does not contribute meaningful information to the ML model. Fig. 5 shows the visualization of the $PS_2[f_i]$ evaluation equation.

$PS_2[f_i]$ can be described with the following equation:

$$PS_2[f_i] = \begin{cases} 1 & \text{if } PV[f_i] > 255 \\ 0 & \text{if } PV[f_i] < 2 \\ 0.5 + (0.5 \times \frac{(PV[f_i]-2)}{(255-2)}) & \text{otherwise} \end{cases}$$

Some might argue that the perturbations in evasion adversarial attacks are minuscule [20], and therefore, the cardinality of the feature should not affect its perturbability. While this may hold true in domains like computer vision, where adversarial perturbations are optimized for human perception and must remain imperceptibly small, it is not the case for network data [23]. In network security, small perturbations often have limited to no utility. In other words, the similarity constraint [24], which ensures that adversarial examples are nearly indistinguishable from the original examples in domains like computer vision, is not applied in the feature-space of attacks against ML-NIDS. Instead, the similarity constraint is placed on the semantics of the attack. Consequently, adversarial attacks in the problem-space can introduce significantly larger perturbations to the features [24]. Moreover, since features are typically normalized or standardized, altering the value of a feature in the problem-space may require even larger perturbations. Thus, the cardinality of a feature becomes a critical factor for an attacker attempting to craft successful evasion adversarial attacks against ML-NIDS in the problem-space.

3.2.3. $PS_3[f_i]$: Correlated Features. This PS field considers the correlation between a NIDS feature and other features. Due to network constraints within NIDS, many features exhibit problem-space correlations. For instance, the flow duration feature is typically correlated with the total forward and backward inter-arrival times. Such correlated features limit the attacker's flexibility. The gradients of the targeted model might recommend a specific perturbation to one feature and a different perturbation to another. However, achieving these opposing perturbations simultaneously is very difficult if the features are highly correlated within the problem-space. As an example, an attacker cannot simultaneously increase the flow duration while decreasing both the forward and backward inter-arrival times. As the number of correlated features associated with a single feature increases, it becomes more difficult to perturb that feature in the problem-space.

$PS_3[f_i]$ will follow a linear function, where its output is 0.5 if the number of Correlated Features (CF) of f_i is equal to or greater than a threshold (the maximum number observed in our experiments was 10, which we chose as the threshold), and 1 if f_i 's CF ($CF[f_i]$) is 0. Fig. 6 shows the visualization of the $PS_3[f_i]$ evaluation equation.

$PS_3[f_i]$ can be described with the following equation:

$$PS_3[f_i] = 1 - 0.05 \times \min(CF[f_i], 10)$$

Handling NIDS feature correlations: The ADAPTIVE-JSMA (AJSMA) attack [23] is an enhanced version of the Jacobian-based Saliency Map Approach (JSMA), specifically adapted for network intrusion detection systems with domain-specific constraints. This attack allows perturbations to be applied in either direction (increasing or decreasing the feature's value), depending on which direction will push the input closer to the target class while adhering to the domain constraints. However, AJSMA focuses on techniques for attacking NIDS at the feature layer, rather than in the problem-space. The complexity of real-world network environments is significantly higher than constraints

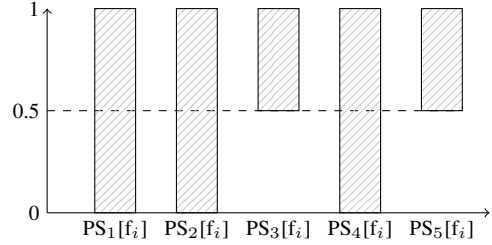


Figure 7. Ranges of PS Fields

modeled in the feature layer, such as protocol-related constraints (TCP, UDP, etc.), which are relatively simple compared to the extensive limitations present in the real-world problem-space like side effect features [8].

Nevertheless, we acknowledge that an attacker could potentially overcome the constraints posed by correlated features in the problem-space, provided they have exceptional knowledge of the attacked ML model and its feature vector. To address this, we implemented a linear function that slightly reduces $PS_3[f_i]$ in the case of two correlated features associated with a single feature. As the number of correlations increases, the function output decreases until it reaches 0.5 (not 0) in the case of 10 correlations, which is the maximum number we have observed. In the worst-case scenario for an attacker (10 correlations or more per feature), the value of $PS_3[f_i]$ will only drop to 0.5, resulting in a modest reduction in $PS_{\text{total}}[f_i]$. However, we still believe that correlated features in the problem-space would pose a significant challenge for an attacker in a practical setting where they have no information about the attacked ML-NIDS and cannot query it. Yet, we opted to only decrease the $PS_{\text{total}}[f_i]$ value, rather than nullify it, to account for the possibility of more advanced future attacks in the problem-space.

3.2.4. $PS_4[f_i]$: Features that attackers cannot access. This PS field focuses on features that attackers cannot access. Examples of such features include backward features (e.g., Minimum Backward Packet Length) and interflow features (e.g., number of flows that have a command in an FTP session (`ct_ftp_cmd`)).

$PS_4[f_i]$'s value will depend on the following conditions:

C3: the feature f_i is not a backward or interflow feature. In other words, attackers can access f_i .

C4: the feature f_i is a backward or interflow feature; however, it is highly correlated with a forward feature. In other words, attackers can modify f_i in an indirect way.

C5: the feature f_i is a backward or interflow feature; however, it is correlated with multiple forward features. In other words, attackers can modify f_i indirectly, but it will be challenging for them as it is correlated with multiple features.

Otherwise (if none of C3, C4, or C5 apply): the feature f_i is a backward or interflow feature and it is not correlated with any forward feature. In other words, attackers cannot access f_i .

$$PS_4[f_i] = \begin{cases} 1, & \text{if (C3 or C4)} \\ 0.5, & \text{if (C5)} \\ 0, & \text{otherwise} \end{cases}$$

3.2.5. $PS_5[f_i]$: Features Correlated with numerous flow Packets. This PS field considers features that are correlated with numerous flow packets.

$PS_5[f_i]$ ’s value will depend on the following condition:

C6: f_i is a feature that requires modifying the entire flow of packets (forward, backward, or both), such as mean or standard deviation features.

$$PS_5[f_i] = \begin{cases} 0.5, & \text{if (C6)} \\ 1, & \text{otherwise} \end{cases}$$

3.2.6. $PS_{Total}[f_i]$. The overall Perturbability Score ($PS_{Total}[f_i]$) for each feature f_i is calculated as the geometric mean of the five individual PS fields we defined. These PS fields are assigned a value of 0 if a specific condition renders feature f_i non-perturbable within the problem-space. A value of 0.5 is assigned if a condition only reduces the feasibility of perturbing f_i . The geometric mean was chosen to ensure that $PS_{Total}[f_i]$ becomes 0 if any of the individual PS fields have a value of 0. However, it’s important to note that any PS field value below 1 will contribute to a decrease in the overall $PS_{Total}[f_i]$.

$PS_{Total}[f_i]$ can be described with the following equation:

$$PS_{Total}[f_i] = \sqrt[5]{\prod_{j=1}^5 PS_j[f_i]}$$

The PS_{Total} will be calculated for all features f_i in the dataset, from $i = 1$ to n , where n is the number of features in the dataset.

3.3. Ranges of PS Fields and Thresholds Calibration

Fig. 7 illustrates the possible ranges of the five PS fields. The ranges for $PS_1[f_i]$, $PS_2[f_i]$, and $PS_4[f_i]$ span from 0 to 1, while $PS_3[f_i]$ and $PS_5[f_i]$ exhibit more restricted ranges, from 0.5 to 1. This variation in the range of PS values reflects the nuanced characteristics of each PS field’s vulnerability to adversarial perturbation.

As previously discussed, the total perturbability score ($PS_{Total}[f_i]$) for each feature f_i is computed as the geometric mean of the five individual PS fields, ensuring a balanced assessment across different conditions. This approach was adopted to account for the fact that certain feature properties can entirely negate their perturbability, such as when the feature is inaccessible to the attacker. These features are given a PS of 0. On the other hand, other conditions may only reduce the feature’s PS without fully eliminating its susceptibility. For instance, features that require altering an entire packet flow—whether forward, backward, or both—such as mean or standard deviation of packet properties, tend to decrease the overall PS score without completely nullifying it. The decision to define varying ranges for different PS fields introduces an implicit weighting mechanism, where each field contributes to the final PS score with varying significance. This differential treatment mirrors real-world scenarios, where certain feature characteristics inherently have a greater influence on the overall perturbability than

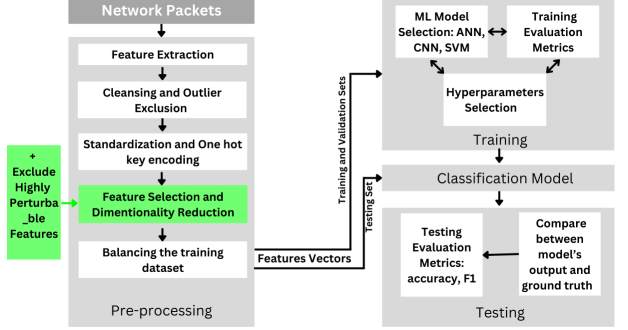


Figure 8. Using PS as a Potential Defense against Practical Problem-Space Evasion Adversarial Attacks

others. Hence, the structured variation in PS field ranges allows for a more precise and context-sensitive evaluation of each feature’s robustness.

While certain thresholds, such as 255 in $PS_2[f_i]$ and 10 in $PS_3[f_i]$, might appear arbitrary at first glance, in the previous section, we provided a detailed rationale for these choices to the best of our ability. These thresholds were selected based on empirical evidence by calibrating PS thresholds against the datasets we used and domain-specific considerations, aiming to balance the practical limitations and the adversarial potential of each feature. However, it is important to recognize that these thresholds, along with the underlying functions of the PS fields, are not set in stone.

As with many design threshold decisions, these parameters and thresholds can—and often should—be calibrated, adapted and fine-tuned by machine learning engineers, domain experts, and practitioners prior to deployment. The flexibility to adjust such thresholds ensures that the perturbability scoring system remains both robust and adaptable to varying real-world scenarios, where the specific characteristics of the network and potential threat models may differ. This adaptability mirrors the iterative nature of system optimization in machine learning pipelines, where parameter tuning plays a pivotal role in enhancing overall performance and security. By allowing these modifications, the PS framework is better equipped to handle the dynamic and evolving landscape of adversarial attacks in network security systems.

3.4. PS as a Defense

Leveraging feature constraints in Network Intrusion Detection Systems offers a promising defense against problem-space adversarial attacks. Fig. 8 presents our novel defense mechanism, which integrates the Perturbability Score (PS) as a key component of the feature selection process.

The development of a Machine Learning-based NIDS (ML-NIDS) begins with network packet data undergoing a rigorous sequence of pre-processing steps. These steps include feature extraction, data cleansing, outlier exclusion, standardization, and one-hot encoding. Once pre-processing is complete, the resulting feature vectors are divided into balanced training sets, as well as validation and testing sets that maintain the original data distribution.

During the training phase, various machine learning models, such as Artificial Neural Networks (ANN), Con-

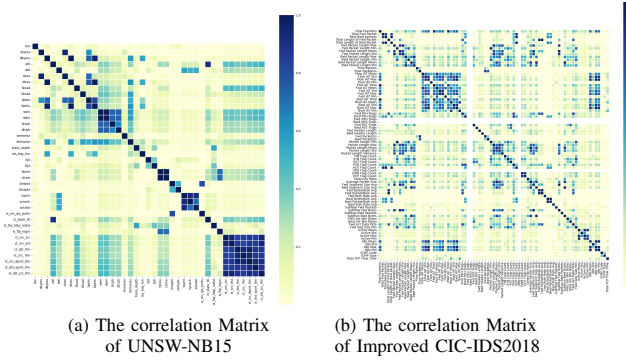


Figure 9. The correlation Matrices between the features in the used datasets, where darker colors mean higher correlation

volutional Neural Networks (CNN), and Support Vector Machines (SVM), are evaluated for performance. Hyperparameter tuning and the selection of training evaluation metrics further optimize these models to ensure robust detection capabilities. In the testing phase, model performance is assessed through accuracy and F1 score metrics, with results compared against ground truth labels to measure the system's robustness and reliability.

A distinguishing aspect of our approach is the exclusion of features with high perturbability scores during the feature selection process. By doing so, attackers encounter no or very few perturbable features in problem-space, significantly reducing the attack surface and making it significantly more difficult for adversaries to exploit the system. This method ensures that the features retained for training and classification are inherently resistant to adversarial manipulations. While this may require rethinking traditional feature selection methods, the potential benefits in preventing evasion attempts are substantial. This simple, efficient solution utilizes NIDS domain constraints as a defense with minimal computational overhead.

4. Experimental Environment

As seen in Fig. 8, the target ML-based NIDS consists of multiple phases. We crafted our own ML-NIDS for our experiments. We will explore our ML-NIDS in the next subsections.

4.1. Datasets

For our experiments, we used 2 public NIDS datasets;

(1) The **UNSW-NB15** dataset [25] is a comprehensive network intrusion detection dataset designed to address the limitations of older benchmarks, such as KDD99 and NSL-KDD [26]. It contains 2,540,044 records, divided into 2,218,761 normal and 321,283 attack samples, spanning 9 different attack categories. The dataset includes 49 features: 47 describing the flow and 2 label features (attack_cat and Label). The UNSW-NB15 features capture various aspects of network behavior, including basic, content, time, and connection-based attributes. It was generated using the IXIA PerfectStorm tool in a controlled testbed environment, simulating both normal network activities and contemporary attack scenarios. This approach ensures that the dataset reflects modern network

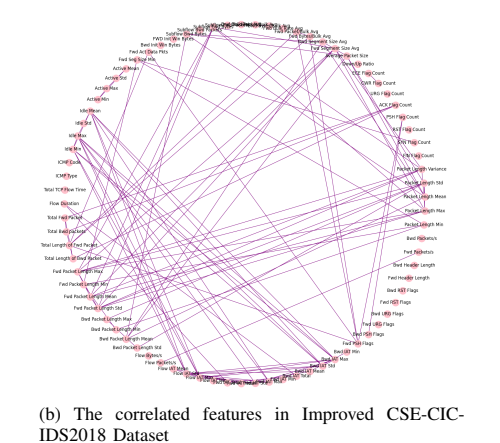
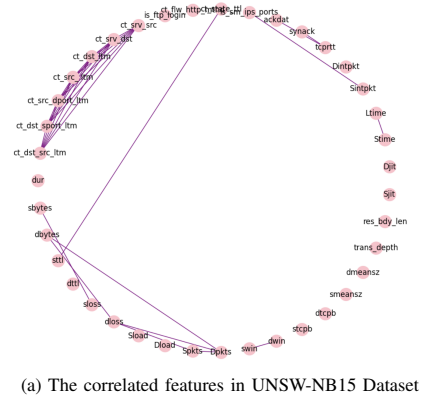


Figure 10. The correlated features in the used datasets

traffic patterns and attack vectors, making it a valuable resource for evaluating and developing network intrusion detection systems in today's cybersecurity landscape.

(2) The **CSE-CIC-IDS2018** dataset [27] is a significant resource for network security research, capturing realistic network traffic over five days and simulating various attack scenarios, including Brute Force, DoS, Botnets, Infiltration, and DDoS, interspersed with benign traffic. With over 80 features extracted from the captured traffic using CICFlowMeter, providing detailed packet and flow-level information, it is widely applicable to machine learning tasks such as classification and anomaly detection. CSE-CIC-IDS2018 is currently one of the most up-to-date datasets and has been shown to improve ML model accuracy in both training and testing [2]. However, recent studies [28] have identified several significant issues related to feature generation and labeling in the CSE-CIC-IDS2018 dataset. Therefore, we utilized the improved version of CSE-CIC-IDS2018 created by Liu et al. [28], which addresses these issues by updating the dataset, modifying the CICFlowMeter Tool, and adding new features like total TCP flow duration, Fwd/Bwd RST flag counts, and support for ICMP protocol.

4.2. Features' Analysis and Correlations

As previously explained, some PS fields depend on the analysis of correlations between the dataset's features. This comprehensive analysis begins by examining the dataset's structure and the number of unique values in each column. A correlation matrix is generated to compute the

TABLE 1. THE NUMBER AND PERCENTAGE OF FEATURES IN EVERY PERTURB-ABILITY CLASS, BASED ON OUR PROPOSED PS, WHERE GREEN INDICATES LOW PERTURB-ABILITY FEATURES CLASS, YELLOW INDICATES MEDIUM PERTURB-ABILITY FEATURES CLASS, AND RED INDICATES HIGH PERTURB-ABILITY FEATURES CLASS

Dataset \ Pert. Class	# and % of Low Pert. Features	# and % of Med. Pert. Features	# and % of High Pert. Features	Total
UNSW-NB15 [25]	26 (55.3%)	4 (8.5%)	17 (36.1%)	47
CSE-CIC-IDS2018* [28]	38 (43.2%)	19 (21.6%)	31 (35.2%)	88

* Improved CSE-CIC-IDS2018 Dataset by Liu et al. [28]

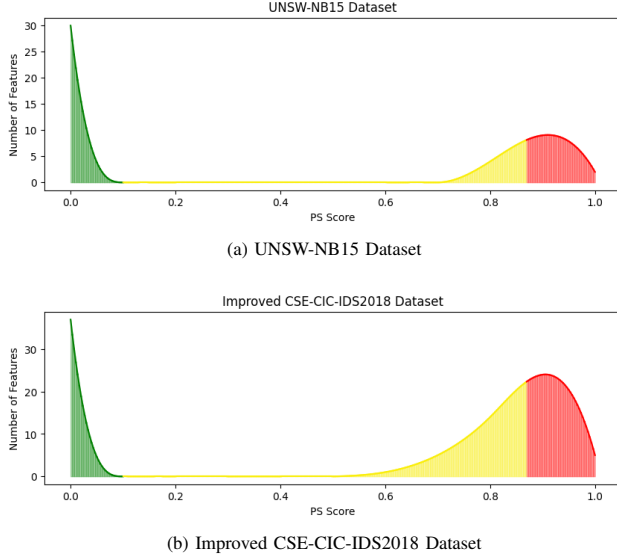


Figure 11. The histogram of PS values for each dataset where green indicates low perturb-ability features class, yellow indicates medium perturb-ability features class, and red indicates high perturb-ability features class

absolute correlations among the remaining features, seen in Fig. 9.

The correlation matrix employs Pearson's correlation coefficient to measure the linear relationship between pairs of features, resulting in values ranging from -1 to 1. A value of 1 indicates a perfect positive linear correlation, -1 indicates a perfect negative correlation, and 0 indicates no correlation. This matrix captures these relationships, facilitating the identification of highly correlated features.

Moreover, we count and report the number of highly correlated features for each feature using the correlation matrix. This step is crucial for $PS_3[f_i]$ calculations. Additionally, a graph representation of the correlation matrix is constructed using NetworkX [29], where nodes represent features and edges denote strong correlations, as seen in Fig. 10. The graph is visualized to illustrate the interconnectedness of highly correlated features, enhancing the understanding of the dataset's structure, which is crucial for the PS architecture and evaluation.

4.3. Pre-processing

The pre-processing algorithm prepares a dataset for machine learning by executing several key steps.

We start by converting all feature columns to numeric format, replacing non-numeric values with NaN, and removing rows with missing values. Identification and non-generalizable features, such as flow ID and timestamps, were also dropped. Our algorithm then separates the fea-

tures from the target variable, encoding the target with a label encoder if it contains categorical data.

One-hot encoding is applied to categorical features. To maintain high model performance with fewer features, we utilized low Pert. (Green) features to extract useful information, such as the region from the destination IP (using the ipapi Python library [30]) and the application from the destination port number. This information is then one-hot encoded before being fed to the models.

Twenty percent of the dataset was allocated for testing. Feature standardization is applied to numerical features, ensuring a mean of zero and a standard deviation of one, enhancing the model's performance. To prevent data leakage, standardization parameters were computed using only the training/validation sets and then applied to the test set. To address class imbalance, we employed random undersampling [31] on the training set to create a balanced dataset.

4.4. Machine and Deep Learning Models

Several ML models were employed to create different versions of our experimental NIDS, enabling more robust comparisons and exploration. The models include a Vanilla Neural Network, a Support Vector Machine (SVM), an ensemble model (Random Forest), and a Deep Learning (DL) model (Convolutional Neural Network, CNN). A detailed description of each follows.

(1) The **Vanilla Neural Network Model** comprises three hidden layers with 64, 32, and 16 neurons, respectively, each employing the ReLU activation function to capture non-linear relationships. The output layer features a single neuron with a sigmoid activation function, suited for binary classification tasks. The model is optimized using the Adam optimizer, minimizing binary cross-entropy loss. The network is trained over 10 epochs with a batch size of 32.

(2) The **SVM model** employs a linear kernel for binary classification. It is trained on the resampled dataset to identify optimal decision boundaries between classes. The linear SVM aims to maximize the margin between support vectors while minimizing classification errors.

(3) The **Random Forest model** consists of an ensemble of 100 decision trees, designed for binary classification tasks. Each tree is trained on a random subset of the data, enhancing the model's robustness and reducing overfitting. The aggregation of predictions from individual trees leads to improved accuracy and stability in classification outcomes. The Random Forest model was also used for feature importance analysis. The model quantifies the contribution of each feature to the model's predictive performance. A DataFrame is created to rank the features and their corresponding importance scores.

(4) The **CNN model** is designed for sequential data classification. The input data is reshaped to accommodate the CNN architecture, with a shape of (samples, timesteps, features). The model consists of a 1D convolutional layer with 64 filters and a kernel size of 3, followed by a max-pooling layer to reduce dimensionality. The flattened output is then passed through a dense layer with 100 neurons and ReLU activation, culminating in an output layer with a softmax activation function to produce class

TABLE 2. UNSW-NB15 DATASET'S FEATURES CLASSIFIED BASED ON OUR PROPOSED PS, WHERE GREEN INDICATES A FEATURE WITH LOW PERTURB-ABILITY, YELLOW INDICATES A FEATURE WITH MEDIUM PERTURB-ABILITY, AND RED INDICATES A FEATURE WITH HIGH PERTURB-ABILITY.

srcip	sport	dstip	dsport	proto	state	dur
sbytes	dbbytes	sttl	dttl	sloss	dloss	service
Sload	Dload	Spkts	Dpkts	swin	dwin	stcpb
dtcpb	smeansz	dmeansz	trans_depth	res_bdy_len	Sjit	Djit
Stime	Ltime	Sintpkt	Dintpkt	tcprrt	synack	ackdat
is_sm_ips_ports	ct_state_ttl	ct_flw_http_mthd	is_ftp_login	ct_ftp_cmd	ct_srv_src	ct_srv_dst
ct_dst_ltm	ct_src_ltm	ct_src_dport_ltm	ct_dst_sport_ltm	ct_dst_src_ltm		

TABLE 3. CSE-CIC-IDS2018 DATASET'S FEATURES CLASSIFIED BASED ON OUR PROPOSED PS, WHERE GREEN INDICATES A FEATURE WITH LOW PERTURB-ABILITY, YELLOW INDICATES A FEATURE WITH MEDIUM PERTURB-ABILITY, AND RED INDICATES A FEATURE WITH HIGH PERTURB-ABILITY.

Flow ID	Src IP	Src Port	Dst IP	Dst Port
Protocol	Timestamp	Flow Duration	Total Fwd Packet	Total Bwd packets
Total Len of Fwd Pack	Total Len of Bwd Pack	Fwd Packet Length Max	Fwd Packet Length Min	Fwd Packet Length Mean
Fwd Packet Length Std	Bwd Packet Length Max	Bwd Packet Length Min	Bwd Packet Length Mean	Bwd Packet Length Std
Flow Bytes/s	Flow Packets/s	Flow IAT Mean	Flow IAT Std	Flow IAT Max
Flow IAT Min	Fwd IAT Total	Fwd IAT Mean	Fwd IAT Std	Fwd IAT Max
Fwd IAT Min	Bwd IAT Total	Bwd IAT Mean	Bwd IAT Std	Bwd IAT Max
Bwd IAT Min	Fwd PSH Flags	Bwd PSH Flags	Fwd URG Flags	Bwd URG Flags
Fwd RST Flags	Bwd RST Flags	Fwd Header Length	Bwd Header Length	Fwd Packets/s
Bwd Packets/s	Packet Length Min	Packet Length Max	Packet Length Mean	Packet Length Std
Packet Len Variance	FIN Flag Count	SYN Flag Count	RST Flag Count	PSH Flag Count
ACK Flag Count	URG Flag Count	CWR Flag Count	ECE Flag Count	Down/Up Ratio
Average Packet Size	Fwd Segment Size Avg	Bwd Segment Size Avg	Fwd Bytes/Bulk Avg	Fwd Packet/Bulk Avg
Fwd Bulk Rate Avg	Bwd Bytes/Bulk Avg	Bwd Packet/Bulk Avg	Bwd Bulk Rate Avg	Subflow Fwd Packets
Subflow Fwd Bytes	Subflow Bwd Packets	Subflow Bwd Bytes	FWD Init Win Bytes	Bwd Init Win Bytes
Fwd Act Data Pkts	Fwd Seg Size Min	Active Mean	Active Std	Active Max
Active Min	Idle Mean	Idle Std	Idle Max	Idle Min
ICMP Code	ICMP Type	Total TCP Flow Time		

probabilities. The model is trained over 10 epochs with a batch size of 32.

5. Results

This section outlines our evaluation plan and details our evaluation scenarios, and presents and discusses the results of our experiments.

5.1. Evaluation Plan for PS

In this subsection, we outline our evaluation plan for the PS metric, focusing on several research questions (RQs) that guide our investigation into the effectiveness and applicability of PS in enhancing the robustness of ML-NIDS;

- **RQ1:** How is the distribution of features characterized using PS? (§5.2)
- **RQ2:** To which PS class do the ML-NIDS features belong? (§5.2)
- **RQ3:** What cutoff is used to differentiate between PS classes? and why was it used? (§5.2)
- **RQ4:** Can ML-NIDS models utilizing only green (low perturb-ability) or a combination of green and yellow (low and medium perturb-ability) features perform as effectively as models that include all features? (§5.3)
- **RQ5:** Does PS effectively capture the easily perturb-able features used in problem-space adversarial attacks against NIDS research? (§5.4)

Through this evaluation plan, we aim to comprehensively assess the utility of the Perturb-ability Score metric in enhancing the robustness of ML-based NIDS, contributing to the ongoing efforts to secure network systems against adversarial threats.

5.2. Classification of the Features Using PS (RQ1,2,3)

Table 1 presents the distribution of features from the two utilized datasets (UNSW-NB15 and the improved CSE-CIC-IDS2018) across different perturbability classes, based on our proposed perturb-ability Score (PS). Features classified as low perturb-ability (green) have a PS of 0, indicating robustness to adversarial manipulation. High perturb-ability features (red) are characterized by a PS greater than or equal to 0.87, marking them as highly perturb-able. We selected the threshold of 0.87 to define highly perturb-able features, as discussed earlier. This threshold is derived from the geometric mean of the five PS components, ensuring that at most one PS field has a value as low as 0.5. In our PS evaluation criteria, a score of 0.5 signifies a condition that tends to reduce the overall PS score, without entirely nullifying it. Using the 0.87 threshold ensures that a feature with at most one such condition is still classified within the high perturb-ability class, thereby reinforcing the rigor of our feature selection criteria.

The remaining features, which are neither in the high nor low perturb-ability classes, fall into the medium perturb-ability class (yellow). Table 1 also shows the percentages of these features across the perturb-ability classes, as defined by our PS. Approximately 35% of the features in both datasets belong to the high perturb-ability class (red).

Fig. 11 depicts the histogram of PS values for each dataset, with the Y-axis representing the number of features and the X-axis representing the PS score. The distribution of PS scores is illustrated, along with the cutoffs between the classes.

TABLE 4. THE PERFORMANCE OF AN ANN/RANDOM FOREST (RF)/SVM/CNN-BASED NIDS

	Dataset →	UNSW-NB15				Improved CSE-CIC-IDS2018			
		Model ↓	Accuracy	Precision	Recall	F1	Accuracy	Precision	Recall
(a) Performance of ML-NIDS with only the low Pert. features (Green) selected during features selection	ANN	0.9879	0.9129	0.9998	0.9544	1.0000	0.9998	0.9998	0.9998
	SVM	0.9879	0.9129	0.9996	0.9543	0.9999	0.9984	0.9994	0.9989
	RF	0.9891	0.9216	0.9986	0.9585	1.0000	0.9997	1.0000	0.9998
	CNN	0.9879	0.9126	0.9999	0.9543	1.0000	0.9993	0.9999	0.9996
(b) Performance of ML-NIDS with only the low and med Pert. features (Green + Yellow) selected during features selection	ANN	0.9879	0.9127	1.0000	0.9543	0.9998	0.9965	1.0000	0.9983
	SVM	0.9879	0.9129	0.9997	0.9543	0.9999	0.9982	0.9998	0.9990
	RF	0.9892	0.9220	0.9987	0.9588	1.0000	0.9998	1.0000	0.9999
	CNN	0.9879	0.9128	1.0000	0.9544	1.0000	0.9996	1.0000	0.9998
(c) Performance of ML-NIDS with all features Pert. (Green + Yellow + Red) selected during features selection	ANN	0.9880	0.9130	0.9999	0.9545	1.0000	0.9996	0.9998	0.9997
	SVM	0.9879	0.9129	0.9997	0.9543	0.9999	0.9983	1.0000	0.9991
	RF	0.9897	0.9251	0.9993	0.9607	1.0000	0.9998	1.0000	0.9999
	CNN	0.9882	0.9145	0.9997	0.9552	1.0000	0.9994	1.0000	0.9997

Table 2 provides a detailed classification of the UNSW-NB15 dataset features according to their perturbability scores. Features such as ‘dstip’ and ‘service’ are categorized as low perturbability (green), implying their robustness against adversarial manipulations. In contrast, features like ‘dur’ and ‘stime’ are identified as high perturbability (red), indicating their susceptibility to adversarial attacks. Table 3 presents the feature classification for the improved CSE-CIC-IDS2018 dataset. Medium perturbability features (yellow), such as ‘Flow Bytes/s’, occupy an intermediate position between these extremes. It is important to note that low perturbability (green) features do not imply that an attacker cannot modify them. Instead, modifying these features may disrupt the network or interfere with the malicious functionality of an attack, or the attacker may have limited or no access to them. Tables 6, 7, and 8 in Appendix A show the definitions of the features in the used datasets.

5.3. Performance of ML-NIDS using various combinations of features based on their perturbability (RQ4)

Table 4 presents the performance of ANN, Random Forest, SVM, and CNN as classifiers in NIDS. The evaluation is conducted on two datasets, with results shown for various feature combinations based on their perturbability. The table is structured into three sections: (a) performance with low perturbability features (green), (b) performance with low and medium perturbability features (green + yellow), and (c) performance with all features (green + yellow + red).

For both datasets, the performance remains consistent across all feature combinations, which is highly promising as it suggests that selecting only low perturbability (green) features can still yield excellent model performance. The improved CSE-CIC-IDS2018 dataset demonstrated outstanding performance across all models, metrics, and feature sets.

Similarly, the UNSW-NB15 dataset performed very well across all models, metrics, and selected features, although precision was slightly lower (but still above 0.912, which is excellent) compared to the other dataset. However, this marginal difference in precision was unrelated to our perturbability-based feature selection. Precision remained consistent across all selected feature sets. Additionally, we ranked the features using Random Forest to select the most important ones, achieving similar precision

results. We also experimented with various balancing techniques, such as SMOTE [32], but observed no significant difference in precision. This consistency further confirms that the precision difference is independent of our perturbability-based feature selection.

In a nutshell, Table 4 shows that using only low perturbability (green) features does not create low-performance models; on the contrary, all of these models have an accuracy and F1 score above 0.9.

It is important to note that in all three cases (a, b, and c) of Table 4, thorough pre-processing was conducted, as discussed in Section §4.3, and feature engineering was applied to remove spurious or faulty features. For example, IP addresses were not treated as numeric values, as this does not generalize well; instead, basic geolocation information was extracted. Time-based features like timestamps were also dropped, as attacks can happen at any time, making this feature non-generalizable. Identification features (e.g., flow ID) were removed for the same reason. Additionally, we applied feature importance ranking techniques to identify the most influential features in the model, ensuring that these attributes provide meaningful and predictive information about the target variable.

5.4. Mapping Traffic Morphing of problem-space attacks to ML-NIDS Features (RQ5)

To validate our proposed PS, we analyzed problem-space evasion adversarial attacks targeting ML-NIDS [11]–[18]. Table 5 presents a detailed mapping of traffic morphing techniques employed in these problem-space adversarial attacks to the corresponding perturbed features within the feature-space of the two datasets utilized in this study. The table outlines the problem-space morphing techniques and maps them to the potentially impacted features. Additionally, it classifies these features according to our perturbability Score (PS) system, using a color-coded scheme: low perturbability (green), medium perturbability (yellow), and high perturbability (red).

In problem-space attacks, the attackers use different methods to morph traffic, which acts like adding perturbations to certain features after feature extraction. For instance, modifying the packet lengths by adding padding affects length-related features, such as the ‘Total Length of Forward Packets’ in the CSE-CIC-IDS2018 dataset. Another example includes increasing the number of packets or altering time-related features, which impacts metrics

TABLE 5. MAPPING PROBLEM-SPACE EVASION ADVERSARIAL ATTACKS' TRAFFIC MORPHING TECHNIQUES TO FEATURES, THE FEATURES ARE COLORED BASED ON OUR PS CLASSIFICATION.*

Problem-space Attack and its Problem-space Morphing Techniques	Potentially Perturb-ed Features in Feature-space in UNSW-NB15	Potentially Perturb-ed Features in Feature-space in improved CSE-CIC-IDS2018
Han et al. [11] modify the interarrival times of packets in the original traffic, change values to the Time to Live (TTL) field, request to establish connections that are already established (or in the process of being established), and add padding to payloads. [11]	sttl, dur, Sjit, Sintpkt, Sload, Stime, Lttime, tcprtt, synack, ackdat . sbytes, smeansz, Sload, dbytes, Dload . Spkts, Dpkts.	Flow Duration, Timestamp, Flow Bytes/s, Flow Packets/s, Fwd IAT Total, Fwd IAT Mean, Fwd IAT Std, Fwd IAT Max, Fwd IAT Min, Fwd Packets/s, .Total Length of Fwd Packet, Fwd Packet Length Max, Min, Fwd Packet Length Mean, Fwd Packet Length Std, Fwd Bulk Rate Avg, Fwd Bytes/Bulk Avg, Fwd Segment Size Avg, Subflow Fwd Bytes , Fwd Act Data Pkts, Total Fwd Packets, Subflow Fwd Packets, Total Bwd Packets, Subflow Bwd Packets . Fwd PSH Flag, Bwd PSH Flags, Fwd URG Flags, Fwd RST Flags, FIN Flag Count, SYN Flag Count, RST Flag Count, PSH Flag Count, ACK Flag Count, URG Flag Count, CWR Flag Count, ECE Flag Count
Hashemi et al. [12] split the original packet payload into multiple packets, modify the timing between packets by either increasing or decreasing the intervals, and inject dummy packets with random lengths, transmission times, and flag settings. [12]	dur, Sjit, Sintpkt, Sload, Stime, Lttime, tcprtt, synack, ackdat . sbytes, smeansz, Sload, dbytes, Dload Spkts, Dpkts.	Flow Duration, Timestamp, Flow Bytes/s, Flow Packets/s, Fwd IAT Total, Fwd IAT Mean, Fwd IAT Std, Fwd IAT Max, Fwd IAT Min, Fwd Packets/s, .Total Length of Fwd Packet, Fwd Packet Length Max, Fwd Packet Length Min, Fwd Packet Length Mean, Fwd Packet Length Std, Fwd Bulk Rate Avg, Fwd Bytes/Bulk Avg, Fwd Segment Size Avg, Subflow Fwd Bytes , Fwd Act Data Pkts, Total Fwd Packets, Subflow Fwd Packets, Total Bwd Packets, Subflow Bwd Packets . Fwd PSH Flag, Bwd PSH Flags, Fwd URG Flags, Fwd RST Flags, FIN Flag Count, SYN Flag Count, RST Flag Count, PSH Flag Count, ACK Flag Count, URG Flag Count, CWR Flag Count, ECE Flag Count
Vitorino et al. [13] [14] [15] modify various flow attributes such as flow duration, average interarrival time between packets, packet rate (packets per second), average forward packet length, smallest forward segment size, minimum interarrival time between packets, and maximum interarrival time. [13] [14] [15]	dur, Sjit, Sload, sbytes, Spkts, Sintpkt smeansz	Flow Duration, Fwd IAT Total, Fwd IAT Mean, Fwd IAT Std, Fwd IAT Max, Fwd IAT Min, Fwd IAT Mean, Fwd IAT Std, Fwd IAT Max, Fwd IAT Min, Fwd Packets/s, .Total Length of Fwd Packet, Fwd Packet Length Max, Fwd Packet Length Min, Fwd Packet Length Mean, Fwd Packet Length Std, Fwd Bulk Rate Avg, Fwd Bytes/Bulk Avg, Fwd Segment Size Avg, Subflow Fwd Bytes , Fwd Act Data Pkts, Total Fwd Packets, Subflow Fwd Packets, Total Bwd Packets, Subflow Bwd Packets . Fwd PSH Flag, Bwd PSH Flags, Fwd URG Flags, Fwd RST Flags, FIN Flag Count, SYN Flag Count, RST Flag Count, PSH Flag Count, ACK Flag Count, URG Flag Count, CWR Flag Count, ECE Flag Count
Yan et al. [16] modify length-related features by padding packets with irrelevant characters, increase the packet count by duplicating the request multiple times, and modify time-related features by introducing delays before each packet is transmitted from the client. [16]	dur, Sjit, Sintpkt, Sload, Stime, Lttime, tcprtt, synack, ackdat . sbytes, smeansz, Sload, dbytes, Dload Spkts, Dpkts.	Flow Duration, Timestamp, Flow Bytes/s, Flow Packets/s, Fwd IAT Total, Fwd IAT Mean, Fwd IAT Std, Fwd IAT Max, Fwd IAT Min, Fwd Packets/s, .Total Length of Fwd Packet, Fwd Packet Length Max, Fwd Packet Length Min, Fwd Packet Length Mean, Fwd Packet Length Std, Fwd Bulk Rate Avg, Fwd Bytes/Bulk Avg, Fwd Segment Size Avg, Subflow Fwd Bytes , Fwd Act Data Pkts, Total Fwd Packets, Subflow Fwd Packets, Total Bwd Packets, Subflow Bwd Packets . Fwd PSH Flag, Bwd PSH Flags, Fwd URG Flags, Fwd RST Flags, FIN Flag Count, SYN Flag Count, RST Flag Count, PSH Flag Count, ACK Flag Count, URG Flag Count, CWR Flag Count, ECE Flag Count
Homoliak et al. [17] spread out packets over time, drop or duplicate packets, rearrange their order, and perform payload fragmentation. [17]	dur, Sjit, Sintpkt, Sload, Stime, Lttime, tcprtt, synack, ackdat . sbytes, smeansz, Sload, dbytes, Dload Spkts, Dpkts.sloss	Flow Duration, Timestamp, Flow Bytes/s, Flow Packets/s, Fwd IAT Total, Fwd IAT Total Mean, Fwd IAT Total Std, Fwd IAT Total Max, Fwd IAT Total Min, Fwd Packets/s, .Total Length of Fwd Packet, Fwd Packet Length Max, Fwd Packet Length Min, Fwd Packet Length Mean, Fwd Packet Length Std, Fwd Bulk Rate Avg, Fwd Bytes/Bulk Avg, Fwd Segment Size Avg, Subflow Fwd Bytes , Fwd Act Data Pkts, Total Fwd Packets, Subflow Fwd Packets, Total Bwd Packets, Subflow Bwd Packets . Fwd PSH Flag, Bwd PSH Flags, Fwd URG Flags, Fwd RST Flags, FIN Flag Count, SYN Flag Count, RST Flag Count, PSH Flag Count, ACK Flag Count, URG Flag Count, CWR Flag Count, ECE Flag Count
Apruzzese et al. [18] morph features related to data transmission by padding UDP packets, and target only TCP packets with the PSH flag by adding small padding to them and repeating the process. [18]	sbytes, smeansz, Sload, dbytes, Dload	Total Length of Fwd Packet, Fwd Packet Length Max, Fwd Packet Length Min, Fwd Packet Length Mean, Fwd Packet Length Std, Flow Bytes/s, Fwd Bulk Rate Avg, Fwd Bytes/Bulk Avg, Fwd Segment Size Avg, Subflow Fwd Bytes , Fwd Act Data Pkts

*Note: The generation of this table is based on our domain knowledge and our understanding of the writings published by the referenced researchers.

like Flow Duration, Total Fwd Packets, and Fwd Inter-Arrival Time (IAT).

As shown in Table 5, the majority of perturbed or affected features in these problem-space evasion attacks exhibit high perturbability scores, classified under the red category. A smaller subset of features shows medium perturbability. This highlights the efficacy of our defense mechanism, which strategically eliminates high-perturbability features, rendering these types of attacks ineffective. Since the attacker manipulates features that are excluded from the final feature set. In other words, our defense will eliminate these easily perturbed features, **which may render these types of attacks ineffective, as the attacker is modifying features that are excluded from the selection, making their changes irrelevant to the feature vector.**

Table 5 highlights a crucial observation: minimal modifications in the problem-space can lead to significant alterations across numerous features in the feature-space.

While this may suggest that attackers possess considerable power or strategic advantage, these manipulations often introduce unintended side effects [24], which we term **collateral damage**.

In practical terms, when an attacker aims to modify a specific feature based on the gradient of the targeted mode, for example, the maximum forward IAT, they might induce a substantial delay between two packets in the flow. However, due to the inherent correlations between features in an ML-based NIDS, this single modification can unintentionally impact a broader set of features. For instance, changing the maximum forward IAT could also affect metrics such as flow duration, packets per second, total forward IAT, and forward IAT mean. This collateral damage does not follow any particular direction of the gradient [1], introducing an element of unpredictability. As a result, these unintentional feature perturbations may negatively influence the success of the attack, potentially undermining the adversary's objectives.

Remark: In Problem-space, there is a huge difference between the affected features, and the features the attacker meant to perturb, there are side effect features (collateral damage).

It is crucial to highlight that while most features can be modified in the problem-space, labeling a feature as non-perturbable means it is difficult to manipulate while **complying with NIDS domain constraints**.

6. Related Work on Conventional Defenses Against Evasion Attacks on ML-NIDS

There are several approaches to defending ML-NIDS against evasion adversarial attacks. He et al. [24] categorize these defense mechanisms into three primary strategies. The first category is *parameter protection techniques*, which aim to conceal the ML model's parameters from adversaries, thereby limiting their ability to exploit model vulnerabilities. An example of this approach is Gradient Masking [33], where the gradient information is obscured to hinder adversarial attacks. The second category includes *adversarial sample detection* methods, which focus on identifying and filtering out adversarial inputs before they can affect the model's performance [34]. The third category encompasses *robustness optimization techniques*, which seek to enhance the resilience of ML models through various strategies. Pre-processing techniques, for instance, aim to eliminate adversarial perturbations before they enter the model. One such technique is Input Randomization [35], where random transformations are applied to input data to obscure potential adversarial modifications. Additionally, adversarial training is a widely recognized method, involving the inclusion of adversarial examples in the training dataset to improve the model's robustness against such attacks [36], [37].

7. Discussion and Lessons Learned

7.1. The Usual Suspects

Through examining and analyzing research on problem-space evasion adversarial attacks [11]–[18], we observed recurring traffic morphing techniques common across numerous attacks. These techniques consistently affect certain features, which we refer to as the **usual suspects**. The usual suspects primarily include Forward IAT, Forward Packet Length, and Forward Payload Size features. Whether our proposed PS method is adopted or not, we believe NIDS researchers should focus on these “usual suspect” features, as modifying them in the problem-space does not compromise the network or the malicious functionality of the adversarial flow.

7.2. Five Features

Sheatsley et al. [23] argued that limiting the number of features an adversary can manipulate does not completely prevent adversarial attacks. Their findings demonstrated that adversarial samples could achieve a 50% success rate by modifying just five randomly selected features.

We would like to point out that our PS-enabled defense does not aim to reduce the number of features but rather to

select features that are non-perturbable **in the problem-space** during the feature selection phase. Thus, the fundamental purpose of our suggested defense is to leave attackers with as few perturbable features as possible (as seen in Table 5, the attackers will likely have access to far fewer than five perturbable features). Moreover, The results by Sheatsley et al. [23] focused on targeting NIDS at the feature layer rather than the problem-space. Real-world network environments are far more complex, and the constraints modeled in their research, such as those related to protocols like TCP and UDP, are a small subset compared to the numerous limitations encountered in the actual problem-space, including side-effect features.

7.3. Problem-space Evasion Adversarial Attacks are Already Extremely Hard for an Attacker

Creating evasion adversarial attacks against ML-NIDS is an extremely complex task for attackers [1]. ElShehaby et al. [1] developed a comprehensive taxonomy of the challenges of adversarial attacks against ML-NIDS. Their exploration of practicality issues spans various attack settings (White- and Black-Box, Feature- and Problem-Space), highlighting challenges such as attackers' access to feature vectors, correlations between NIDS features, the impractical assumption that attackers have detailed knowledge of the model and feature extraction techniques or can query ML-NIDS, and the added complexity introduced by the dynamic nature of modern ML-NIDS.

Focusing on problem-space evasion attacks, these typically begin with perturbations in the feature-space. These manipulations are then translated into real-world modifications of network packets, a challenge known as the Inverse Feature-Mapping Problem [8]. This issue creates a substantial obstacle for attackers, often complicating, and in many cases preventing, the straightforward application of gradient-based feature-space attacks to generate problem-space adversarial examples [8]. Additionally, there is no guarantee that an optimal solution in the problem-space will closely resemble the intended adversarial features [24]. Furthermore, early efforts to identify mutation operations relied heavily on trial and error, offering little to no theoretical guidance [24]. He et al. [24] also reported in their survey that the evaluations of adversarial attacks they reviewed predominantly focus on the evasiveness of the attacks rather than their maliciousness. In other words, current adversarial attack research against NIDS does not prioritize maintaining the malicious nature of the flow after problem-space modifications. Moreover, Some problem-space perturbations are counterproductive. For instance, introducing delays between packets to perturb IAT features in DoS (Denial-of-Service) attacks can undermine the attack's effectiveness, as the reduced packet rate would make the attack more manageable and less disruptive.

Thus, introducing a simple addition in the feature-selecting phase in the architecture of ML-NIDS through the usage of the PS scoring mechanism to eliminate easily perturbable features could be the last nail in the coffin for these already highly impractical and complex problem-space evasion adversarial attacks against NIDS. Furthermore, in real-world adversarial attacks, guessing often plays a pivotal role [10]. In the NIDS domain,

adversaries typically lack access to the attacked model’s internal information and cannot directly query the target system. As a result, they may need to predict the selected features of the target system [1]. If these selected features are unpredictable and difficult to perturb within the problem-space, attackers will be significantly constrained in crafting effective adversarial examples.

7.4. Feature Reduction as a Defense Against Adversarial Attacks

Previous works have explored feature squeezing or reduction as a defense mechanism against adversarial attacks by narrowing the search space available for attackers [13] [3]. While this approach aims to limit the attack surface, our defense strategy goes beyond mere feature removal. Instead of simply reducing the feature set, we leverage domain-specific constraints to identify and select inherently robust features, using PS. These features are carefully chosen based on their resilience to perturbations, where modifications are likely to compromise the malicious or network functionality of evasion adversarial attacks targeting NIDS. By focusing on features that are not easily perturbed without causing significant operational side effects, our approach offers a more effective defense against problem-space adversarial attacks on NIDS. This makes it much more difficult for attackers to succeed without violating network constraints or compromising their malicious capability.

7.5. NIDS Datasets

We acknowledge that current NIDS datasets exhibit numerous issues, including poor data diversity, highly dependent features, unclear ground truth, traffic collapse, artificial diversity, and incorrect labels [38]. To address these challenges, we utilized the improved version of CSE-CIC-IDS2018 created by Liu et al. [28]. They identified several significant issues related to feature generation and labeling in the original dataset and addressed these by modifying the CICFlowMeter Tool and adding new features. Furthermore, we implemented thorough data pre-processing techniques to maximize the utility of these datasets and prevent data leakage. However, it is important to note that our aim was not to evaluate NIDS datasets but rather to compare the performance of the best model with access to the entire feature set against the best model utilizing only non-perturb-able features.

7.6. We are losing information!

Some may argue that utilizing PS to drop certain features could result in the loss of information that may be important for the ML-NIDS. While this concern is valid, it is essential that the application of PS be guided by architects, practitioners, and engineers with substantial domain knowledge. On the other hand, our results might suggest that current literature might be utilizing more information and features than necessary. Table 4 presents promising results with only the green features. Another pertinent question is: why rely on features that are easily perturb-able by an outsider?

7.7. Adversarial Attacks on ML-NIDS Research Direction

During our exploration for this work, we observed common issues in research on adversarial attacks against NIDS. Many studies are overly generous to the attacker, often assuming access to information that is rarely available in real-world settings. Grosse et al. [9] noted that this issue is common across artificial intelligence security applications research generally.

In the NIDS domain, many research studies on evasion adversarial attacks presume full knowledge of the model and its selected feature set, which is not feasible in practice. Moreover, research on black-box evasion adversarial attacks assumes the possibility of querying ML-NIDS, which is likely to be infeasible in real-world scenarios [1]. As established in this paper, problem-space adversarial attacks are more practical than feature-space attacks. However, even for these attacks, existing evaluations tend to focus on their evasiveness rather than their maliciousness [24]. Additionally, research on problem-space adversarial attacks against ML-NIDS has largely overlooked the impact of side effects/collateral damage features [24]. There are also considerable issues within NIDS datasets that must be addressed [38].

8. Conclusion

This paper investigates the perturb-ability of features within NIDS by introducing the Perturb-ability Score (PS) metric. A high PS indicates that a feature is easily manipulated in the problem-space while maintaining the malicious and network functionality of the modified flow, while a low PS suggests that altering that feature may either be infeasible or could render the network flow or malicious objective invalid. Through our research, we have leveraged the PS as a potential defense mechanism against practical problem-space evasion adversarial attacks by selectively identifying and utilizing features with low PS. This novel strategy introduces a fresh approach, utilizing NIDS domain constraints to mitigate the impact of adversarial attacks on ML-based network intrusion detection systems.

The results from our experiments demonstrate that discarding features with high PS does not compromise model performance. Instead, it enhances the robustness of NIDS against adversarial threats, providing reliable detection capability. The findings suggest that by focusing on inherently robust features, we can effectively fortify NIDS against problem-space evasion adversarial attacks while maintaining high detection accuracy.

Overall, this work presents a promising avenue for enhancing the security of ML-based NIDS. Future research will focus on further refining the PS metric and exploring its applicability across different datasets and attack scenarios, ultimately contributing to the development of more resilient network security systems.

References

[1] M. e. Shehaby and A. Matrawy, “Adversarial evasion attacks practicality in networks: Testing the impact of dynamic learning,” *arXiv preprint arXiv:2306.05494*, 2023.

[2] Z. Ahmad, A. Shahid Khan, C. Wai Shiang, J. Abdullah, and F. Ahmad, “Network intrusion detection system: A systematic study of machine learning and deep learning approaches,” *Transactions on Emerging Telecommunications Technologies*, vol. 32, no. 1, p. e4150, 2021.

[3] O. Ibitoye, R. Abou-Khamis, A. Matrawy, and M. O. Shafiq, “The threat of adversarial attacks on machine learning in network security—a survey,” *arXiv preprint arXiv:1911.02621*, 2019.

[4] A. E. Cinà, K. Grosse, A. Demontis, S. Vascon, W. Zellinger, B. A. Moser, A. Oprea, B. Biggio, M. Pelillo, and F. Roli, “Wild patterns reloaded: A survey of machine learning security against training data poisoning,” *ACM Computing Surveys*, vol. 55, no. 13s, pp. 1–39, 2023.

[5] A. Saha, A. Subramanya, and H. Pirsiavash, “Hidden trigger backdoor attacks,” in *Proceedings of the AAAI conference on artificial intelligence*, vol. 34, no. 07, 2020, pp. 11957–11965.

[6] M. Juuti, S. Szylner, S. Marchal, and N. Asokan, “Prada: protecting against dnn model stealing attacks,” in *2019 IEEE European Symposium on Security and Privacy (EuroS&P)*. IEEE, 2019, pp. 512–527.

[7] B. Biggio, I. Corona, D. Maiorca, B. Nelson, N. Šrndić, P. Laskov, G. Giacinto, and F. Roli, “Evasion attacks against machine learning at test time,” in *Machine Learning and Knowledge Discovery in Databases: European Conference, ECML PKDD 2013, Prague, Czech Republic, September 23–27, 2013, Proceedings, Part III 13*. Springer, 2013, pp. 387–402.

[8] F. Pierazzi, F. Pendlebury, J. Cortellazzi, and L. Cavallaro, “Intriguing properties of adversarial ml attacks in the problem space,” in *2020 IEEE symposium on security and privacy (SP)*. IEEE, 2020, pp. 1332–1349.

[9] K. Grosse, L. Bieringer, T. R. Besold, and A. M. Alahi, “Towards more practical threat models in artificial intelligence security,” in *33rd USENIX Security Symposium (USENIX Security 24)*, 2024, pp. 4891–4908.

[10] G. Apruzzese, H. S. Anderson, S. Dambra, D. Freeman, F. Pierazzi, and K. Roundy, ““real attackers don’t compute gradients”: bridging the gap between adversarial ml research and practice,” in *2023 IEEE Conference on Secure and Trustworthy Machine Learning (SATML)*. IEEE, 2023, pp. 339–364.

[11] D. Han, Z. Wang, Y. Zhong, W. Chen, J. Yang, S. Lu, X. Shi, and X. Yin, “Evaluating and improving adversarial robustness of machine learning-based network intrusion detectors,” *IEEE Journal on Selected Areas in Communications*, vol. 39, no. 8, pp. 2632–2647, 2021.

[12] M. J. Hasbani, G. Cusack, and E. Keller, “Towards evaluation of nids in adversarial setting,” in *Proceedings of the 3rd ACM CoNEXT Workshop on Big DAta, Machine Learning and Artificial Intelligence for Data Communication Networks*, 2019, pp. 14–21.

[13] J. Vitorino, I. Praça, and E. Maia, “Sok: Realistic adversarial attacks and defenses for intelligent network intrusion detection,” *Computers & Security*, p. 103433, 2023.

[14] —, “Towards adversarial realism and robust learning for iot intrusion detection and classification,” *Annals of Telecommunications*, vol. 78, no. 7, pp. 401–412, 2023.

[15] J. Vitorino, N. Oliveira, and I. Praça, “Adaptative perturbation patterns: Realistic adversarial learning for robust intrusion detection,” *Future Internet*, vol. 14, no. 4, p. 108, 2022.

[16] H. Yan, X. Li, W. Zhang, R. Wang, H. Li, X. Zhao, F. Li, and X. Lin, “Automatic evasion of machine learning-based network intrusion detection systems,” *IEEE Transactions on Dependable and Secure Computing*, vol. 21, no. 1, pp. 153–167, 2023.

[17] I. Homoliak, M. Teknos, M. Ochoa, D. Breitenbacher, S. Hosseini, and P. Hanacek, “Improving network intrusion detection classifiers by non-payload-based exploit-independent obfuscations: An adversarial approach,” *arXiv preprint arXiv:1805.02684*, 2018.

[18] G. Apruzzese, A. Fass, and F. Pierazzi, “When adversarial perturbations meet concept drift: an exploratory analysis on ml-nids,” 2024.

[19] N. Carlini and D. Wagner, “Towards evaluating the robustness of neural networks,” in *2017 ieee symposium on security and privacy (sp)*. Ieee, 2017, pp. 39–57.

[20] I. J. Goodfellow, J. Shlens, and C. Szegedy, “Explaining and harnessing adversarial examples,” *arXiv preprint arXiv:1412.6572*, 2014.

[21] G. Apruzzese, M. Andreolini, L. Ferretti, M. Marchetti, and M. Collajanni, “Modeling realistic adversarial attacks against network intrusion detection systems,” *Digital Threats: Research and Practice (DTRAP)*, vol. 3, no. 3, pp. 1–19, 2022.

[22] M. El Shehaby and A. Matrawy, “The impact of dynamic learning on adversarial attacks in networks (ieee cns 23 poster),” in *2023 IEEE Conference on Communications and Network Security (CNS)*. IEEE, 2023, pp. 1–2.

[23] R. Sheatsley, N. Papernot, M. J. Weisman, G. Verma, and P. McDaniel, “Adversarial examples for network intrusion detection systems,” *Journal of Computer Security*, vol. 30, no. 5, pp. 727–752, 2022.

[24] K. He, D. D. Kim, and M. R. Asghar, “Adversarial machine learning for network intrusion detection systems: a comprehensive survey,” *IEEE Communications Surveys & Tutorials*, 2023.

[25] N. Moustafa and J. Slay, “Unsw-nb15: a comprehensive data set for network intrusion detection systems (unsw-nb15 network data set),” in *2015 military communications and information systems conference (MilCIS)*. IEEE, 2015, pp. 1–6.

[26] R. Bala and R. Nagpal, “A review on kdd cup99 and nsl nsl-kdd dataset,” *International Journal of Advanced Research in Computer Science*, vol. 10, no. 2, 2019.

[27] I. Sharafaldin, A. H. Lashkari, and A. A. Ghorbani, “Toward generating a new intrusion detection dataset and intrusion traffic characterization,” *ICISSp*, vol. 1, pp. 108–116, 2018.

[28] L. Liu, G. Engelen, T. Lynar, D. Essam, and W. Joosen, “Error prevalence in nids datasets: A case study on cic-ids-2017 and cse-cic-ids-2018,” in *2022 IEEE Conference on Communications and Network Security (CNS)*. IEEE, 2022, pp. 254–262.

[29] “Networkx,” <https://networkx.org/>, 2024, accessed: 2024-10-10.

[30] “ipapi,” <https://pypi.org/project/ipapi/>, 2024, accessed: 2024-10-10.

[31] B. Liu and G. Tsoumakas, “Dealing with class imbalance in classifier chains via random undersampling,” *Knowledge-Based Systems*, vol. 192, p. 105292, 2020.

[32] N. V. Chawla, K. W. Bowyer, L. O. Hall, and W. P. Kegelmeyer, “Smote: synthetic minority over-sampling technique,” *Journal of artificial intelligence research*, vol. 16, pp. 321–357, 2002.

[33] A. Nayebi and S. Ganguli, “Biologically inspired protection of deep networks from adversarial attacks,” *arXiv preprint arXiv:1703.09202*, 2017.

[34] R. Feinman, R. R. Curtin, S. Shintre, and A. B. Gardner, “Detecting adversarial samples from artifacts,” *arXiv preprint arXiv:1703.00410*, 2017.

[35] C. Xie, J. Wang, Z. Zhang, Z. Ren, and A. Yuille, “Mitigating adversarial effects through randomization,” *arXiv preprint arXiv:1711.01991*, 2017.

[36] R. Abou Khamis and A. Matrawy, “Evaluation of adversarial training on different types of neural networks in deep learning-based idss,” in *2020 international symposium on networks, computers and communications (ISNCC)*. IEEE, 2020, pp. 1–6.

[37] R. Abou Khamis, M. O. Shafiq, and A. Matrawy, “Investigating resistance of deep learning-based ids against adversaries using min-max optimization,” in *ICC 2020-2020 IEEE International Conference on Communications (ICC)*. IEEE, 2020, pp. 1–7.

[38] R. Flood, G. Engelen, D. Aspinall, and L. Desmet, “Bad design smells in benchmark nids datasets,” in *2024 IEEE 9th European Symposium on Security and Privacy (EuroS&P)*. IEEE, 2024, pp. 658–675.

Appendix A.

Definition of Features of UNSW-NB15 and improved CSE-CIC-IDS2018 Datasets

TABLE 6. THE FEATURES DESCRIPTION OF THE UNSW-NB15 DATASET

Feature	Description
srcip	Source IP address
sport	Source port number
dstip	Destination IP address
dsport	Destination port number
proto	Transaction protocol
state	Indicates to the state and its dependent protocol, e.g. ACC, CLO, CON, ECO, ECR, FIN, I NT, MAS, PAR, REQ, RST, TST, TXD, URH, URN, and (-) (if not used state)
dur	Record total duration
sbytes	Source to destination transaction bytes
dbytes	Destination to source transaction bytes
sttl	Source to destination time to live value
ttl	Destination to source time to live value
sloss	Source packets retransmitted or dropped
dloss	Destination packets retransmitted or dropped
service	http, ftp, smtp, ssh, dns, ftp-data ,irc and (-) if not much used service
Sload	Source bits per second
Dload	Destination bits per second
Spkts	Source to destination packet count
Dpkts	Destination to source packet count
swin	Source TCP window advertisement value
dwin	Destination TCP window advertisement value
stcpb	Source TCP base sequence number
dtcpb	Destination TCP base sequence number
smeansz	Mean of the packet size transmitted by the src
dmeansz	Mean of the packet size transmitted by the dst
trans_depth	Represents the pipelined depth into the connection of http request/response transaction
res_bdy_len	Actual uncompressed content size of the data transferred from the server's http service.
Sjit	Source jitter (mSec)
Djit	Destination jitter (mSec)
Stime	record start time
Ltime	record last time
Sintpkt	Source interpacket arrival time (mSec)
Dintpkt	Destination interpacket arrival time (mSec)
tcprrt	TCP connection setup round-trip time, the sum of 'synack' and 'ackdat'.
synack	TCP connection setup time, the time between the SYN and the SYN_ACK packets.
ackdat	TCP connection setup time, the time between the SYN_ACK and the ACK packets.
is_sm_ips_ports	If source (1) and destination (3)IP addresses equal and port numbers (2)(4) equal then, this variable takes value 1 else 0
ct_state_ttl	No. for each state (6) according to specific range of values for source/destination time to live (10) (11).
ct_flw_http_mthd	No. of flows that has methods such as Get and Post in http service.
is_ftp_login	If the ftp session is accessed by user and password then 1 else 0.
ct_ftp_cmd	No of flows that has a command in ftp session.
ct_srv_src	No. of connections that contain the same service (14) and source address (1) in 100 connections according to the last time (30).
ct_srv_dst	No. of connections that contain the same service (14) and destination address (3) in 100 connections according to the last time (30).
ct_dst_ltm	No. of connections of the same destination address (3) in 100 connections according to the last time (30).
ct_src_ltm	No. of connections of the same source address (1) in 100 connections according to the last time (30).
ct_src_dport_ltm	No of connections of the same source address (1) and the destination port (4) in 100 connections according to the last time (30).
ct_dst_sport_ltm	No of connections of the same destination address (3) and the source port (2) in 100 connections according to the last time (30).
ct_dst_src_ltm	No of connections of the same source (1) and the destination (3) address in 100 connections according to the last time (30).

TABLE 7. THE FEATURES DESCRIPTION OF THE CSE-CIC-IDS2018 DATASET (PART A)

Feature	Description
Flow ID	The id of the flow
Src IP	Source IP address
Src Port	Source port number
Dst IP	Destination IP address
Dst Port	Destination port number
Protocol	Transaction protocol
Timestamp	record start time
Flow Duration	Flow duration
Total Fwd Packet	Total packets in the forward direction
Total Bwd packets	Total packets in the backward direction
Total Length of Fwd Packet	Total size of packet in forward direction
Total Length of Bwd Packet	Total size of packet in backward direction
Fwd Packet Length Max	Maximum size of packet in forward direction
Fwd Packet Length Min	Minimum size of packet in forward direction
Fwd Packet Length Mean	Average size of packet in forward direction
Fwd Packet Length Std	Standard deviation size of packet in forward direction
Bwd Packet Length Max	Maximum size of packet in backward direction
Bwd Packet Length Min	Minimum size of packet in backward direction
Bwd Packet Length Mean	Mean size of packet in backward direction
Bwd Packet Length Std	Standard deviation size of packet in backward direction
Flow Bytes/s	flow byte rate that is number of bytes transferred per second
Flow Packets/s	flow packets rate that is number of packets transferred per second
Flow IAT Mean	Average time between two flows
Flow IAT Std	Standard deviation time two flows
Flow IAT Max	Maximum time between two flows
Flow IAT Min	Minimum time between two flows
Fwd IAT Total	Total time between two packets sent in the forward direction
Fwd IAT Mean	Mean time between two packets sent in the forward direction
Fwd IAT Std	Standard deviation time between two packets sent in the forward direction
Fwd IAT Max	Maximum time between two packets sent in the forward direction
Fwd IAT Min	Minimum time between two packets sent in the forward direction
Bwd IAT Total	Total time between two packets sent in the backward direction
Bwd IAT Mean	Mean time between two packets sent in the backward direction
Bwd IAT Std	Standard deviation time between two packets sent in the backward direction
Bwd IAT Max	Maximum time between two packets sent in the backward direction
Bwd IAT Min	Minimum time between two packets sent in the backward direction
Fwd PSH Flags	Number of times the PSH flag was set in packets travelling in the forward direction (0 for UDP)
Bwd PSH Flags	Number of times the PSH flag was set in packets travelling in the backward direction (0 for UDP)
Fwd URG Flags	Number of times the URG flag was set in packets travelling in the forward direction (0 for UDP)
Bwd URG Flags	Number of times the URG flag was set in packets travelling in the backward direction (0 for UDP)
Fwd RST Flags	Number of times the RST flag was set in packets travelling in the forward direction
Bwd RST Flags	Number of times the RST flag was set in packets travelling in the backward direction
Fwd Header Length	Total bytes used for headers in the forward direction
Bwd Header Length	Total bytes used for headers in the backward direction
Fwd Packets/s	Number of forward packets per second
Bwd Packets/s	Number of backward packets per second
Packet Length Min	Minimum length of a flow
Packet Length Max	Maximum length of a flow
Packet Length Mean	Mean length of a flow
Packet Length Std	Standard deviation length of a flow
Packet Length Variance	Minimum inter-arrival time of packet
FIN Flag Count	Number of packets with FIN
SYN Flag Count	Number of packets with SYN
RST Flag Count	Number of packets with RST
PSH Flag Count	Number of packets with PUSH
ACK Flag Count	Number of packets with ACK
URG Flag Count	Number of packets with URG
CWR Flag Count	Number of packets with CWE
ECE Flag Count	Number of packets with ECE
Down/Up Ratio	Download and upload ratio
Average Packet Size	Average size of packet

TABLE 8. THE FEATURES DESCRIPTION OF THE CSE-CIC-IDS2018 DATASET (PART B)

Feature	Description
Fwd Segment Size Avg	Average size observed in the forward direction
Bwd Segment Size Avg	Average size observed in the backward direction
Fwd Bytes/Bulk Avg	Average number of bytes bulk rate in the forward direction
Fwd Packet/Bulk Avg	Average number of packets bulk rate in the forward direction
Fwd Bulk Rate Avg	Average number of bulk rate in the forward direction
Bwd Bytes/Bulk Avg	Average number of bytes bulk rate in the backward direction
Bwd Packet/Bulk Avg	Average number of packets bulk rate in the backward direction
Bwd Bulk Rate Avg	Average number of bulk rate in the backward direction
Subflow Fwd Packets	The average number of packets in a sub flow in the forward direction A subflow is a TCP connection which can have different internet path identified by IP addresses of source and destination network interfaces.
Subflow Fwd Bytes	The average number of bytes in a sub flow in the forward direction
Subflow Bwd Packets	The average number of packets in a sub flow in the backward direction
Subflow Bwd Bytes	The average number of bytes in a sub flow in the backward direction
FWD Init Win Bytes	Number of bytes sent in initial window in the forward direction
Bwd Init Win Bytes	# of bytes sent in initial window in the backward direction
Fwd Act Data Pkts	# of packets with at least 1 byte of TCP data payload in the forward direction
Fwd Seg Size Min	Minimum segment size observed in the forward direction
Active Mean	Mean time a flow was active before becoming idle
Active Std	Standard deviation time a flow was active before becoming idle
Active Max	Maximum time a flow was active before becoming idle
Active Min	Minimum time a flow was active before becoming idle
Idle Mean	Mean time a flow was idle before becoming active
Idle Std	Standard deviation time a flow was idle before becoming active
Idle Max	Maximum time a flow was idle before becoming active
Idle Min	Minimum time a flow was idle before becoming active
ICMP Code	Internet Control Message Protocol Code
ICMP Type	Internet Control Message Protocol Type
Total TCP Flow Time	Total TCP Flow Time